Photoproduction of $\pi^0\pi^0$ on proton and deuteron with the rescattering mechanism $\pi^+\pi^- \to \pi^0\pi^0$ inclusion

Mikhail Egorov

Laboratory of Mathematical Physics, Tomsk Polytechnic University, 634050 Tomsk, Russia

E-mail: egorovphys@mail.ru

Abstract. The model of coherent $\pi^0\pi^0$ mesons photoproduction on simplest nuclei of hydrogen and deiterium in the region $E_\gamma \leq 1.4$ GeV is presented. Two pion rescattering amplitude in process $\pi^+\pi^- \to \pi^0\pi^0$ is taken into account from phenomenological fit is accurately defined in threshold region as well as up to 1100 MeV of relative energy in $\pi\pi$ c.m. Strong dependence of the result on the rescattering amplitude is also discussed.

1. Introduction

Photoproduction of neutral pions is an effective instrument for nuclear structure investigation. The reason for the keep interest to these reactions is the absence of relationship among photons and neutral mesons thereby strong background contributions (like as $\Delta-$Kroll-Ruderman, meson pole term) vanished in neutral π photoproduction processes. Consequently nucleon resonance contributions plays general role in final $\pi^0 N$ channel.

Double pion photoproduction processes in such a manner should be emphasized as an indicator of availability nucleon excitations decaying into two pion channel. Therein neutral channel $\pi^0\pi^0$ for that total cross sections on proton and deuteron are precisely measured is seen is more experimentally studied.

However, these experimental data is theoretically indescribable nowadays. Authors [1, 2, 3, 4] are used different models for reaction amplitude as a rule, due to that fact real reaction mechanism for $\pi^0\pi^0$ final state can not to be reproduced. The deficiency of authoritative predictions for total cross section on proton in $\pi^0\pi^0$ channel is usually seen to be original anzats of double neutral pions photoproduction model is used on more complicated nuclei and processes.

The amplitude investigation problem for $\pi^0\pi^0$ channel can be precisely solved in corresponding partial wave analysis procedure. However, this procedure is hard enough and partially done for a restricted number of partial waves $J = 3/2$ [5] in the near threshold region. In accordance with these qualitative data for total cross sections of $(\gamma, \pi^0\pi^0)$ on light nuclei should be already informative enough. The main idea being in comparison cross sections are to be obtained on nuclei with different spin and isotopical spin, concludes about contributions of intermediate mechanisms into one body photoproduction operator.

Against the problem of $(\gamma, \pi^0\pi^0)$ amplitude interpenetration mentioned above the contribution of process $\pi\pi \to \pi\pi$ with rescattering into neutral channel should be also bear in mind. In double pion photoproduction reactions in resonance region rescattering $\pi\pi \to \pi\pi$ process is considered to be meager. It can be only emphasized work [6], in which rescattering

effect is analyzed with essential approximations. More precisely $\pi\pi$ interaction is considered in inelastic pion scattering $\pi^- p \to \pi^0\pi^0 n$ process [7] and in N-N collisions $NN \to \pi\pi NN$ [8].

An influence of $\pi\pi$ rescattering on maximum location in $d\sigma/d\omega_{\pi\pi}$ distribution had been detected a few years ago in photoproduction of two pions on complex nuclei [9, 10, 11]. Nevertheless from phenomenology methods used in work in progress it does not estimate the magnitude of rescattering mechanism in total cross sections.

For to estimate corresponding rescattering effect in $\pi^0\pi^0$ photoproduction processes on light nuclei corresponding amplitude $T_{\pi\pi}$ was taken into account from analyze [12]. Following the analyze amplitude parametrization leads to well reproduction of $\pi\pi$ phase shifts and corresponds to dispersive summation rules. In order to simplified calculations for $T_{\pi\pi}$ amplitude evaluation in present work we are restricted by only $s-$wave part.

2. The model of $\gamma N \to \pi^0\pi^0 N$.

Let us consider cross section of $\gamma N \to \pi^0\pi^0 N$ reaction in total center-of-mass system. Unpolarized total cross section is given by

$$d\sigma = (2\pi)^{-5}\frac{M_N^2}{8W^2\omega_\gamma}q_\pi^* p_f \frac{1}{8}\sum_{\lambda\, M_i M_f}\left|T^\lambda_{M_i,M_f}\right|^2 d\omega_{\pi\pi}d\Omega_{\mathbf{q}^*}d\Omega_{\mathbf{p_f}}\,, \tag{1}$$

where M_N-nucleon mass, $W-$total energy of the system and $w_\gamma-$photon energy in reaction center-of-mass. It is convenient to use kinematic variables, corresponding to two pions like as momentum of a pion in center-of-mass of both pions q_π^* and related with its solid angle $\Omega_{\mathbf{q}*}$, for to differential cross section (1) getting.

Invariant mass of $\pi\pi$ system is labeled by $\omega_{\pi\pi}$, final nucleon momentum and corresponding solid angle are defined by p_f and $\Omega_{\mathbf{p_f}}$. In wave function calculation for fermions and bosons we use the following normalization achieved in analyze [13]. Matrix element $T^\lambda_{M_i\,M_f} = \langle M_f \mid \hat{T}^\lambda_{\gamma N} \mid M_i\rangle$ (1) is defined as transition between nucleon statement with spin $J = 1/2$ and M_i, M_f as its projections, in which photon helicity is labeled by $\lambda = \pm 1$.

In one-body photoproduction operator $\hat{T}^\lambda_{\gamma N}$ calculation we use standard scheme [4]. Namely phenomenological Lagrangians with Borns and resonance contributions calculated on tree level (see Fig. (1)) are used. More precisely multiply rescattering in $\pi - N$ and $\pi - \pi$ subsystems are effectively taken into account due to nucleon resonances (diagrams (7)-(9) on Fig.(1)) and meson resonances (diagrams $(4), (7), (17)$ on Fig.(1)) inclusion. For resonance's terms final two pion state is seen to be a result of decay of intermediate quasi-two-body $\pi - \Delta$ and $\sigma - N$ states. Following this idea, one-body photoproduction operator is given in the form

$$\hat{T}_{\gamma N} = \hat{T}^B_{\gamma N} + \hat{T}^{\pi\Delta}_{\gamma N} + \hat{T}^{\sigma N}_{\gamma N}\,, \tag{2}$$

where $\hat{T}^B_{\gamma N}$ includes all Born terms (diagrams (1)-(6), (10)-(16) see Fig.(1)), $\hat{T}^{\pi\Delta}_{\gamma N}$ and $\hat{T}^{\sigma N}_{\gamma N}$ corresponds resonance's excitation with intermediate $\pi - \Delta$ and $\sigma - N$ states. Some of the details of one-body operator (2) is seen in work [4] in particular damping factors and t-channel propagator of the diagram number (4) shown on Fig.(1). Here we will briefly describe some specific patterns of the present model. As an another resonance nucleon excitations (black boxes on Fig.(1)) are originally excluded in work [4] we calculate $\Delta(1600)P^{\star\star\star}_{33}$, $N(1700)D_{13}$, $N(1650)S_{11}$, $\Delta(1905)F_{35}$, $\Delta(1910)P_{31}$, $N(1720)P_{13}$. Contribution of $N(1720)P_{13}$ in cited work is considered only in quasi-two-body channel with πN as a intermediate state. For the simplicity contribution all of these additional resonance terms will be labeled by *a.c.* on figures and in text. Hadron and electromagnetic radiation coupling constants based on partial amplitudes $A_{1/2}$ and $A_{3/2}$ meanings are known in PDG-2014 [14] compilation and are came from averaged hadron radiation decay widths of intermediate resonance states. Role of relative phase shifts among

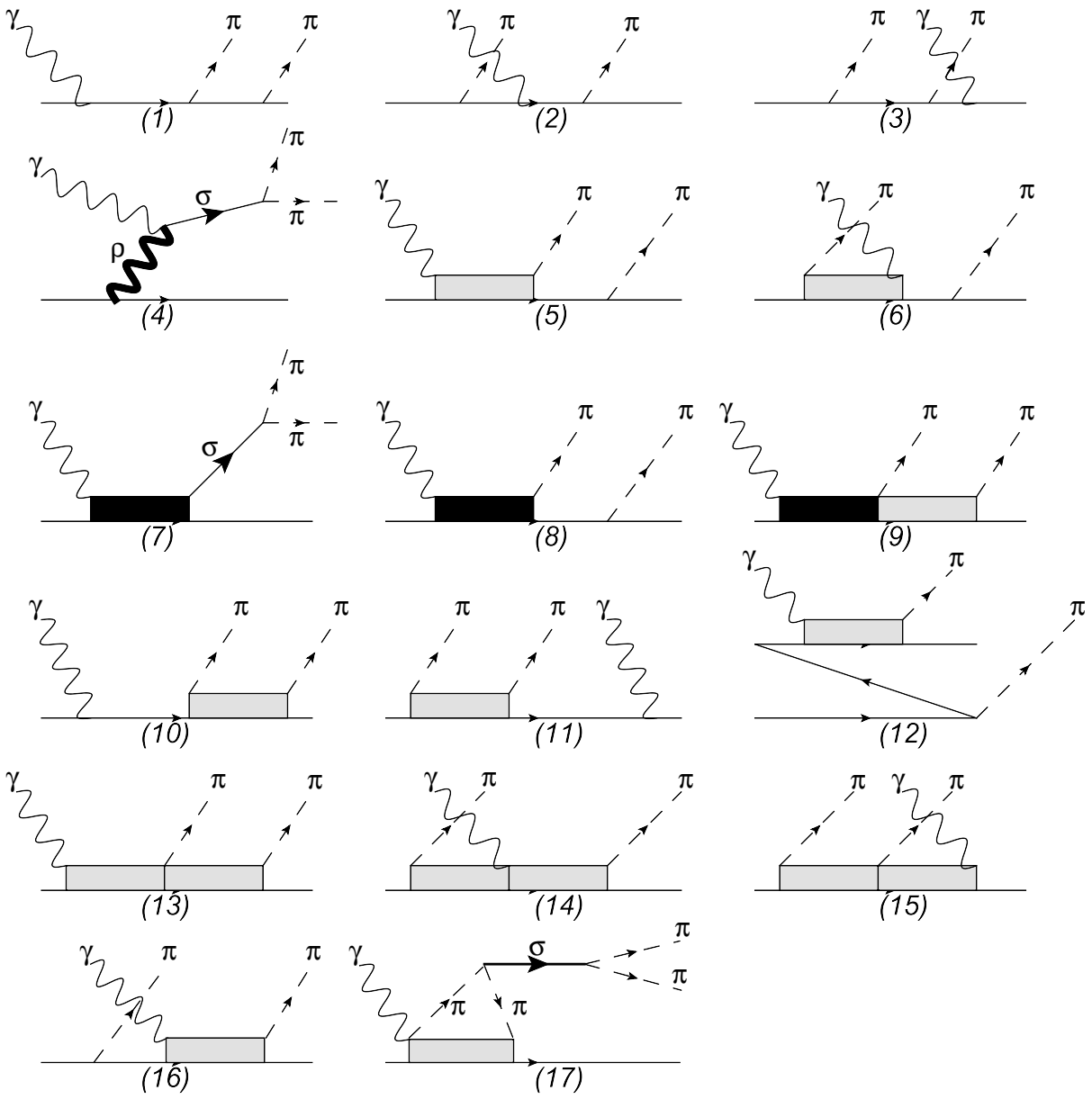

Figure 1. Diagrams (1-6), (10-16) $N-$ and $\Delta-$Born terms for $N(\gamma,\pi^0\pi^0)N$ process, (7-9)-resonance terms, with hadron couplings defined in Tab.(1). Diagram (17) corresponds to rescattering process $\pi^+\pi^-\to\pi^0\pi^0$, is considered in the work.

additive components of (2) for diagrams shown on Fig.(1) is neglected. However, for some hadron couplings signs were taken into account in coincidence with partial wave analyze of work [15] for $\pi N\to\pi\pi N$ process. Generally, calculation of hadron radiation couplings (see Tab.(1)) is similar to that in [4], with that difference, e.g., in $D_{13}(1520)$ and $F_{15}(1680)$ resonances modern helicity amplitudes and hadron decay widths are used.

In deuteron case photoproduction operator of $\pi^0\pi^0$ mesons should also contains two-body contribution part, corresponding electromagnetic inputs into amplitude (2) of two nucleons. However, in present work we neglect such effects and are concentrated only on the impulse

Table 1. Coupling constants for baryon resonances used in the work. Coupling $f_{\pi NN}$ is found on relativized isobar model base, in which $f^2_{\pi NN}/4\pi = 0.08$. Coupling ρNN is defined according to work [27], averaging the meaning $g^2_\rho/4\pi = 2$. As coupling constants $\gamma\rho\sigma$, σNN the corresponding meanings from work [4] are used. Meson-baryon constants are in modulus. Line means the absence of valid values for that decay channel in PDG [14]. In parentheses wave numbers for the channel in progress are presented. In columns with electromagnetic constants g^M and g^E for resonances with isospin $T = 1/2$ two meanings – isoscalar and isovector components of amplitude (2) are shown. Underlined cells in first column corresponds to additional in relative to model [4] resonance contributions in $\pi^0\pi^0$ channel.

N^*	$f_{\pi NN^*}$	$f_{\pi\Delta N^*}$	$f_{\rho NN^*}$	$f_{\sigma NN^*}$	g^M	g^E
N	1.0	2.08	5	10.02	$-0.06/1.85$	
$\Delta(1232)P_{33}$	2.1	3.8	–	–	-1.81	-0.067
$\underline{\Delta(1600)P_{33}}$	0.48	1.97	17.5(p)	–	-0.086	0.09
$\underline{N(1520)D_{13}}$	0.29	0.7(s)/0.7(d)	2.7	1.86	0.58/0.85	-0.027/0.22
$\underline{N(1700)D_{13}}$	0.08	1.75(s)/0.09(d)	1.8	–	0.07/0.08	-0.012/-0.007
$\underline{N(1680)F_{15}}$	0.07	0.4(p)/0.1(f)	6.0(p)/22.4(f)	1.6	0.53/1.45	0.20/0.24
$N(1440)P_{11}$	1.1	3.4	23.7	5.4	0.07/0.36	
$\Delta(1700)D_{33}$	0.1	1.9(s)/0.3(d)	3.4(s)/21.1(d)	–	-0.50	0.24
$\underline{N(1650)S_{11}}$	1.5	0.4	1.65	0.9		-0.05/ -0.087
$\underline{N(1535)S_{11}}$	1.2	0.37	1.27(s)	1.0		-0.05/-0.16
$\underline{\Delta(1905)F_{35}}$	0.02	0.5(p)/0.04(f)	7.5(p)	–	-0.60	-0.087
$\underline{\Delta(1910)P_{31}}$	0.34(p)	0.8	–	–	-0.016	
$\underline{N(1720)P_{13}}$	0.26(p)	1.3(p)	19.5(p)	–	-0.06/-0.030	-0.025/0.020
$\underline{N(1675)D_{15}}$	0.16	0.6(d)/0.05(g)	5.8	36.4(f)	-0.22/0.43	-0.03/-0.05
$\Delta(1620)S_{31}$	0.8	0.8	2.7	–		-0.07

character of $\gamma - d$ interaction. Deuteron wave function has the form

$$\Psi_{M_S\,M_d}(\vec{p}) = \sum_{L\,M_L} C^{1M_d}_{LM_L\,1M_S}\, u_L(p)\, Y_{LM_L}(\hat{p}) \mid 0\,0\rangle \mid 1\ M_S\rangle\,, \tag{3}$$

in which M_S and M_d are spin projections of two final nucleons and initial deuteron correspondingly. Isospin and spin wave functions, including into Eq.(3) are labeled by $\mid 0\,0\rangle$ and $\mid 1M_S\rangle$, correspondingly. Momentum $\vec{p}$ characterizes the relative motion of two nucleons in deuteron.

A sum in Eq. (3) is realized by means of orbital momentum L, equals 0 and 2 for the deuteron and its projection M_L. As radial deuteron wave function component $u_L(p)$ we use effective enough in a wide photon energy region up to $E_\gamma \leq 800$ MeV one [16] is famous for its simplicity. Total cross section for the $d(\gamma,\pi^0\pi^0)pn$ process, averaged over deuteron and final two nucleon spins and also summarized over photon helicity has the form

$$d\sigma = (2\pi)^{-8}\frac{E_d M_N^2}{8W^2\omega_\gamma} q^*_\pi p^*_N Q \frac{1}{12} \sum_{\lambda\,M_d,S,M_S} \left|T^\lambda_{IM_i\,SM_S\,\lambda M_d}\right|^2 d\omega_{\pi\pi} d\omega_{NN} d\Omega_{\mathbf{q}^*} d\Omega_{\mathbf{p}^*_\mathbf{N}} d\Omega_\mathbf{Q}\,. \tag{4}$$

Total momentum of two pions is labeled through $\mathbf{Q}$ in this equation. In two nucleon sector invariant mass ω_{NN} and momentum of a nucleon in both nucleon's center-of-mass system $\mathbf{p}^*_N$ are introduced. Furthermore matrix element in Eq.(4) in contrast to Eq.(1), is also depends on

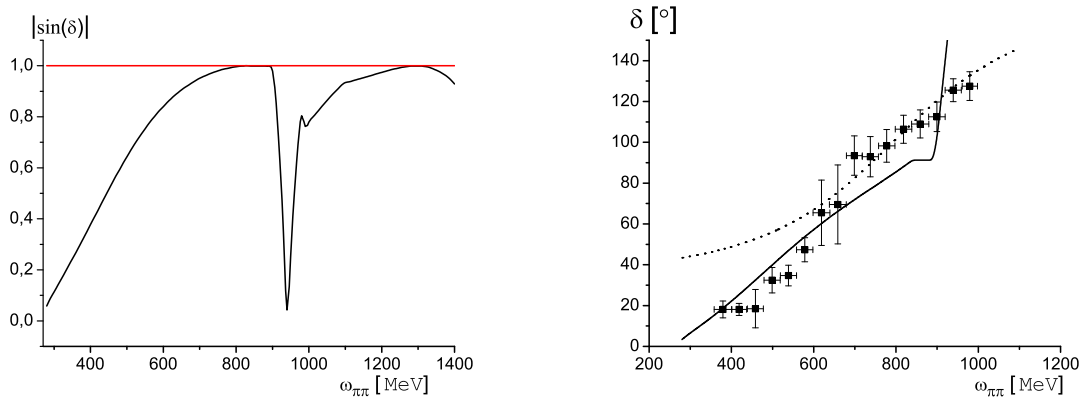

Figure 2. Phase shifts for partial wave of pions scattering with zero orbital momentum and isospin, calculated with model [12]. Left panel: modulus of sinus of phase shifts δ, corresponding to partial wave of $\pi\pi$ system with zero isospin and orbital momentum. Right panel: solid curve – phase shift δ in comparison with experimental data [17]; dotted curve corresponds to calculation of phase shifts δ with amplitude (11).

final two nucleon momentum relative to center-of-mass of reaction. We neglect corresponding momentum denotation in Eq.(4) for the simplicity.

Nevertheless it should be also emphasized a remark respective to kinematic variables, calculated in two pions and two nucleons sectors correspondingly. Role of these new in this sense variables adds up to simplicity of cross sections (1) and (4) calculations, is in definition of kinematic for both two pions and two nucleons sectors with following Lorenz transformation into running system.

For process $d(\gamma,\pi^0\pi^0)pn$ matrix element $T^{\lambda}_{IM_i\,SM_S\,\lambda M_d}$ is a sum of one-body photoproduction $\pi^0\pi^0$ operators sandwiched between deuteron and final two nucleons wave functions

$$T^{\lambda}_{IM_i\,SM_S\,\lambda M_d} = \langle SM_S; IM_I \mid T^{\lambda}_{\gamma N_1} + T^{\lambda}_{\gamma N_2} \mid 1M_d; 0\,0\rangle\,. \tag{5}$$

In Eqs.(4-5) spin and isospin of final nucleons are denoted by SM_S and IM_I, correspondingly. Nevertheless, following Pauli antisymmetrization principle for final nucleons, the permutation of two nucleon momenta is followed by summation (4) of matrix elements in Eq.(5) with sign multiplier $(-1)^{S+I}$.

In coherent process $d(\gamma,\pi^0\pi^0)d$ matrix element (5) is sandwiched by deuteron wave functions $\mid 1M_d; 0\,0\rangle$. The later, of course, admits the transitions that do not changes nucleon isospin projection. It this regard matrix element calculation for coherent process is less complicated in contrast to (5), because of, e.g., in one-body operator following Born diagrams (5), (6), (12), (13), (15), (16) (see Fig. (1)) are excluded. At the same time in calculation of total cross section on deuteron in coherent process $(\gamma,\pi^0\pi^0)$ it should be excluded baryon resonances with isospin $T = 3/2$ at all, like as general contribution of rescattering process (diagram (17) see Fig.(1)).

3. Rescattering mechanism $\pi^+\pi^- \to \pi^0\pi^0$

On Fig.(2) modulus of $\sin\delta$, where $\delta-$shift if partial wave with zero orbital momentum and isopsin is seen. At the same figure it is shown comparison of calculated $s-$wave phase shifts with experimental data of the work [17]. As it can be seen from the figure present model phase shift calculation is in good accordance with experimental data for the elastic $\pi^0\pi^0$ scattering.

In terms of relativistic calculation rescattering effect $\pi^+\pi^- \to \pi^0\pi^0$ is introduced via usual loop integration over momentum $\mathbf{q}'$. Integral is evaluated over multiplication of two pion's

propagators, T-matrix of charge pions production T^{γ} (in of that for the simplicity we drop spin's subscripts here and in continuous) and invariant T-matrix of rescattering mechanism $T_{\pi\pi}$.

In rescattering process shown on the diagram (17) (see Fig.(1)) appropriate form factor defined off-shell behavior of $T_{\pi\pi}$ amplitude should be also included in photoproduction operator. Corresponding equation for diagram (17) has the form

$$T_R^{\gamma} = \int \frac{1}{4\omega_{\pi'}} \frac{d^3q'}{(2\pi)^3} T^{\gamma} F(\Lambda, q^2, q'^2) T_{\pi\pi} \frac{-1}{\omega_{\pi}^2 - \omega_{\pi'}^2} \,. \tag{6}$$

In Eq.(6) ω_{π} is on-shell energy of a pion. Energy of another one $\omega_{\pi'}$ is off shell and given by

$$\omega_{\pi}^2 - \omega_{\pi'}^2 = \mathbf{q}_{\pi}^2 - \mathbf{q}_{\pi'}^2 + i0 \,, \tag{7}$$

where $i0$ is infinite small complex parameter.

Relationship among amplitude $f_{\pi\pi}$ of the process $\pi\pi \to \pi\pi$ with invariant T-matrix included in (6) is given by

$$T_{\pi\pi} = 16\pi\sqrt{\omega_{\pi}\omega_{\pi'}}\sqrt{\frac{q}{q'}} f_{\pi\pi} \,. \tag{8}$$

Integration in Eq.(6) with pole term decomposition leads equation

$$T_R^{\gamma} = \frac{(\exp(2i\delta(q)) - 1)}{2} \left(T^{\gamma}(q) + \frac{\sqrt{\omega_{\pi}}}{i\pi q\sqrt{q}} P \int_0^{\infty} \frac{T^{\gamma}(q') q'^2 \sqrt{q'} F(\Lambda, q^2, q'^2) d\, q'}{\sqrt{\omega_{\pi'}}(\omega_{\pi}^2 - \omega_{\pi'}^2)} \right), \tag{9}$$

in which direct dependence of T-matrix of charge pion production on momenta q and q' is seen. Principle value of integral in Eq.(9) is denoted by $P\int\cdots$. In order to take into account off-shell nature of double pion production in calculation (6) following form-factor is used

$$F(\Lambda, q^2, q'^2) = \frac{\Lambda^2 + q^2}{\Lambda^2 + q'^2} \,, \tag{10}$$

Making up the use of (10) cut off parameter Λ is equal to 650 MeV.

It should be emphasized, that as a charge pion production mechanism in diagram (17) (see Fig.(1)) in calculation we evaluate the process $N(\gamma, \pi^+\pi^-)N$. Invariant T-matrix T^{γ} for that process is taken into account with the non relativistic model [4] approach.

Inclusion of pion rescattering mechanism into one-body operator of neutral $\pi^0\pi^0$ pair production is realized by addition $\hat{T}_R^{\gamma}$ in Eq.(2).

Resulting cross sections obtained in such a manner are shown on Figs.(4, 5, 6).

Rescattering effect in total cross section of the process $p(\gamma, \pi^0\pi^0)p$ calculated with Eq.(6), in which charge pair production T-matrix T^{γ} is defined by non relativistic isobar model [4] slightly depends on the off-shell part of the $f_{\pi\pi}$ amplitude (see solid line on the right pannel of Fig.(3)). This off-shell effect is seen in the region of photon energy $E_{\gamma} \approx 500$ MeV, where its meaning defines more one half of total cross section. Calculation of the rescattering mechanism with the Eq.(9) where principle value of the integral is omitted is shown by dashed curve on Fig.(3).

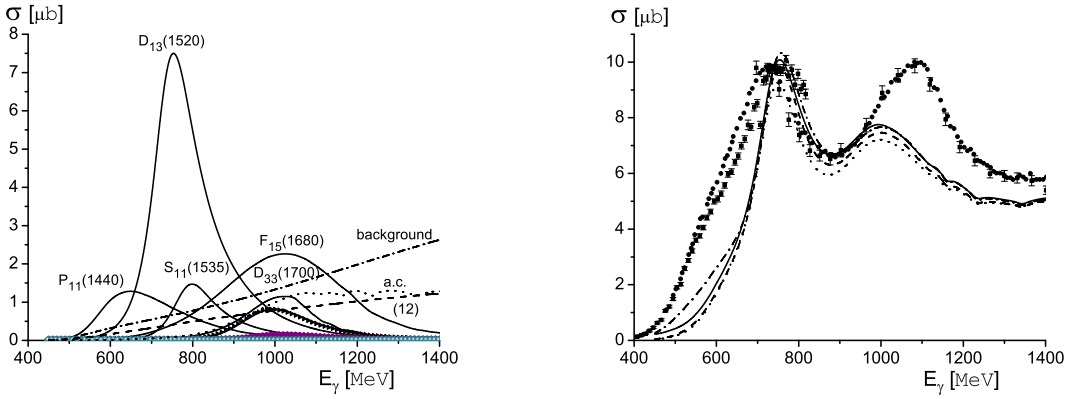

Figure 3. Left: resonance proton excitations. Dashed line corresponds to diagram (12); dash-dotted line denotes sum of $N-$ and $\Delta-$Born terms (see Fig.(1)). Dotted line corresponds to *a.c.* Contribution of $S_{11}(1650)$ resonance is labeled by black triangles. Contribution of other sizable resonances is labeled on the figure. Lines for the $F_{35}(1905)$, $S_{31}(1680)$, $D_{15}(1625)$, $D_{13}(1700)$ resonances merges with axe. Right: total cross section of the $p(\gamma,\pi^0\pi^0)p$ process. Dotted curve denotes plane wave calculation. Solid curve corresponds to rescattering effect inclusion (see diagram (17) on the Fig.(1)) amplitude of that defined in the work [12] with form-factor from Eq.(10). Dashed curve denotes only pole term contribution in Eq.(9). Dash-dotted curve corresponds to rescattering effect with the use of Eq.(11) calculated with Eq.(12). Experimental data: circles [20], squares [21].

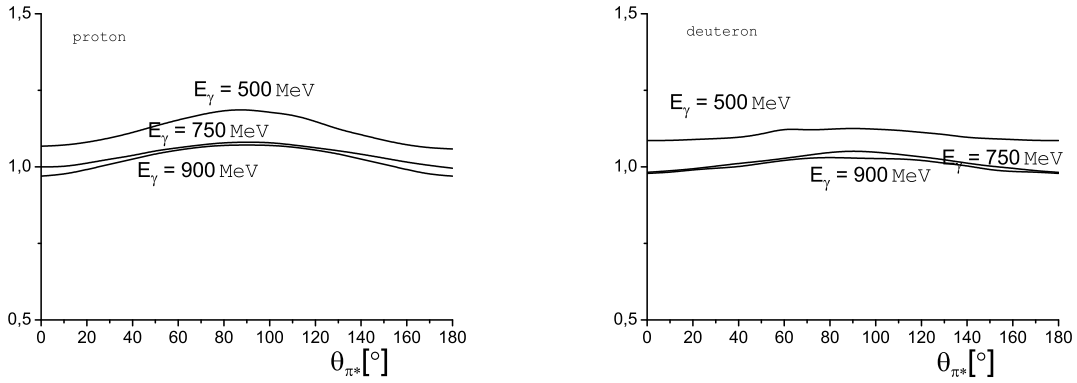

Figure 4. Ratio of differential distributions $\frac{d\sigma(PW+\pi\pi)/d\Omega_{\pi^*}}{d\sigma(PW)/d\Omega_{\pi^*}}$, calculated with three fixed photon energies, with $(PW+\pi\pi)$ and without (PW) pion rescattering mechanism in process $p(\gamma,\pi^0\pi^0)p$ (left) and $d(\gamma,\pi^0\pi^0)pn$ (right).

4. Results and discussion

Contributions of separate resonances in total cross section $p(\gamma,\pi^0\pi^0)p$, calculated with the model [4] usage, in which we are introduced coupling constants shown on Tab.(1), and also additional resonance and Born terms denoted in one of the previous section as *a.c.* , are presented on Fig.(3).

It is necessary to emphasized the role of baryon resonances $D_{33}(1700)$ $S_{11}(1650)$, $P_{13}(1720)$. If decay of last two resonances in $\pi\Delta$ channel is omitted in work [4], then according to the

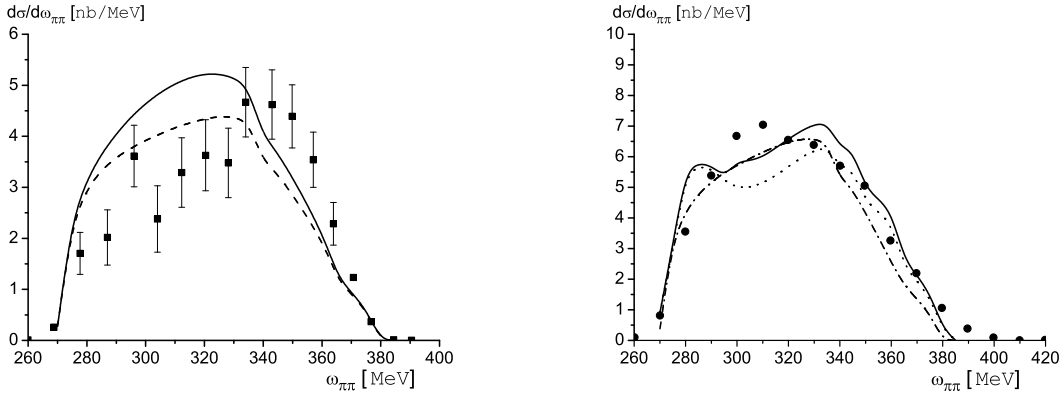

Figure 5. Differential cross section $d\sigma/d\omega_{\pi\pi}$ for reaction $p(\gamma,\pi^0\pi^0)p$ (left) and $d(\gamma,\pi^0\pi^0)pn$ (right). Dashed curves: plane wave calculations; solid curves: rescattering effect inclusion (see diagram (17) on Fig.(1)) with Eq.(9) in which only pole term is kept in mind. Dotted curve on right panel is a sum of two differential distributions on proton and neutron. Experimental data: [22] (proton), [23] (deuteron).

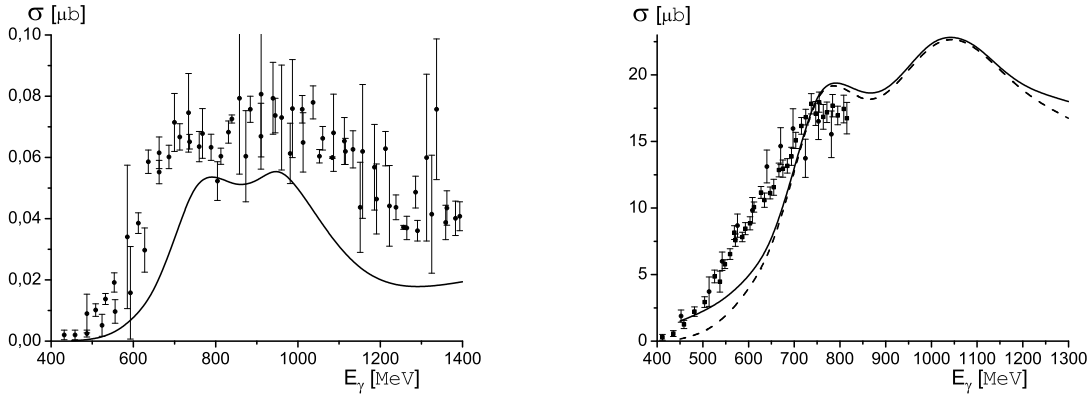

Figure 6. Total cross section for process $d(\gamma,\pi^0\pi^0)d$ (left) and $d(\gamma,\pi^0\pi^0)pn$ (right). Dashed (solid) curve on right (left) panel corresponds plane wave calculations. Solid curve on right panel corresponds rescattering effect icnlusion with Eq.(12). Preliminary experimental data for $d(\gamma,\pi^0\pi^0)d$ process [24], and data for the process $d(\gamma,\pi^0\pi^0)pn$: circles [25], squares [26].

Fig.(3) contribution of $S_{11}(1650)$ resonances is of the same magnitude as $S_{11}(1535)$ in $\pi\Delta$ channel. At the same time the volume of $D_{33}(1700)$ is increased that, however, does not mean the sizable [18] role this resonances in second and third resonance region. It should be pointed out the negligible role of *a.c.* terms, are also considered in present work. Role of these terms get only increase in $E_\gamma > 1000$ MeV region. Behavior of baryon resonances $D_{13}(1520)$, $P_{11}(1440)$, $F_{15}(1680)$, in general, is in accordance with analyze [4]. Finally, the summarized contribution of baryon resonances $F_{35}(1905)$, $S_{31}(1680)$, $D_{15}(1625)$, $D_{13}(1700)$ is shown by shaded area in photon energy region $E_\gamma \approx 1000 - 1100$ MeV.

In total cross section of $p(\gamma,\pi^0\pi^0)p$ the enhancement of coincidence with experiment is seen. Among the others characteristics of present calculation from [4] it should be noted more precise reconstitution of cross section minimum at $E_\gamma = 800-950$ MeV (see Fig. (3)). At the same time

rescattering mechanism inclusion, in which process amplitude $\pi\pi \to \pi\pi$ is taken into account from [12], and only pole in Eq.(9) term is kept is negligible in total cross section. Nevertheless total effect from Eq.(9), as it has already mentioned above, defines more then a half of total cross section of $p(\gamma, \pi^0\pi^0)p$ process in the photon energy region $E_\gamma \approx 500$ MeV.

There are interest enough to compare two result for rescattering effect $\pi\pi \to \pi\pi$ calculated on the one hand side with usage the fit [12] and with Breit-Wigner parametrization for the rescattering amplitude $f_{\pi\pi}$ on the other hand. It is known the later has the following form

$$f_{\pi\pi} = -\frac{m_\sigma \Gamma_\sigma}{q\,(\omega^2_{\pi\pi} - m^2_\sigma + i\Gamma_\sigma m_\sigma)}\,. \tag{11}$$

The σ meson decay width Γ_σ and its mass m_σ are fitting parameters of pion's scattering task, formulated in terms of scalar-isoscalar σ resonance (σ meson) production and its decay. In this regard it is convenient enough to reproduce these fitting parameters from description of $s-$wave phase shifts of $\pi\pi$ scattering. Taken into account in such a manner $\pi\pi$ scattering $s-$wave phase shifts δ has been shown on Fig.(2) by dotted curve. In present calculation of $\pi\pi \to \pi\pi$ with Breit-Wigner's amplitude (11) we use $m_\sigma = 740$ MeV and $\Gamma_\sigma = 600$ MeV, had also been reproduced by the work [6].

Pole term decomposition in integral (6) with the substitution of Eq.(8) and Eq.(11) leads to formulas

$$T^\gamma_R = \frac{m_\sigma \Gamma_\sigma}{\omega^2_{\pi\pi} - m^2_\sigma + i\Gamma_\sigma m_\sigma}\left(- iT^\gamma(q) - \frac{\sqrt{\omega_\pi}}{\pi q\sqrt{q}} P \int\limits_0^\infty \frac{T^\gamma(q') q'^2 \sqrt{q'} F(\Lambda, q^2, q'^2) d\,q'}{\sqrt{\omega_{\pi'}}(\omega^2_\pi - \omega^2_{\pi'})}\right). \tag{12}$$

In Eq.(12), as like as in Eq.(9) T-matrix of charge pion production T^γ has the evident momentum dependence on q and q'.

Rescattering effect calculation with Eq.(12) where the priciple value is omitted is seen by dash-dotted curve on Fig.(3). It can be conclude the general effect came from diagram (17) (see Fig.(1)) with Eq.(12) is in $E_\gamma = 500 - 550$ MeV region from the figure.

To illustrate how the rescattering effect depends on the polar angle of a pion motion θ_{π^*} in both pions $\pi^0\pi^0$ center-of-mass system it is also calculated the ratio

$$\frac{d\sigma_{\pi\pi}(E^i_\gamma)/d\Omega_{\pi^*}}{d\sigma(E^i_\gamma)/d\Omega_{\pi^*}},\ where\, E^i_\gamma\ =\ 500,\ 750,\ 900\, MeV\,, \tag{13}$$

in which $d\sigma_{\pi\pi}(E^i_\gamma)/d\Omega_{\pi^*}(d\sigma(E^i_\gamma)/d\Omega_{\pi^*})$–differential distribution of $\pi^0\pi^0$ production with (without) pion rescattering mechanism, calculated on three photon energies meanings. It should be notice the fact in calculation $d\sigma_{\pi\pi}(E^i_\gamma)/d\Omega_{\pi^*}$ in Eq.(9) the principle value is omitted.

Resulting ration (13) with all things mentioned above is shown in Fig.(4). As it can be seen from the figure, the study of the behavior of (13) in processes $p(\gamma, \pi^0\pi^0)p$ and $d(\gamma, \pi^0\pi^0)pn$ is identical from the polar angle θ_{π^*} and photon energy E_γ dependence. The existence of mild maximum in the region $\theta_{\pi^*} = 90^\circ$ in both presented on Fig.(4) processes at $E_\gamma = 500$ implicitly supports the role of rescattering effect in that kinematic region where both of them are oppositely distributed point of view. The almost the same behavior has already mentioned in work [19] for coherent $\pi\pi$ processes on ^{12}C nucleus. As it can be seen from the Fig.(4), in general, photon energy increase followed by rescattering effect drop in a wide polar angle θ_{π^*} region.

It should be emphasized the problem related with the Eq.(6) usage. Due to the fact T-matrix of charge pion production T^γ, defined from [4], is assigned in restricted kinematic region corresponding to on-shell distribution all of intermediate $\pi\Delta$, ρN and σN states of process $N(\gamma, \pi^+\pi^-)N$. In these regard it is expected the integration over loop $\mathbf{q}'$ momentum leads to

uncontrolled effect in total cross section. Actually inclusion of T^{γ} into integration in Eqs.(9), (12) leads almost ten times increasing of $d\sigma/d\omega_{\pi\pi}-$distributions (not shown on the figures) in a wide invariant mass $\omega_{\pi\pi}$ region. Moreover the form of the ratio (13) is also changed while the effect in total cross section (see Fig. (3)) is negligible.

On the Fig.(5) differential cross sections $d\sigma/d\omega_{\pi\pi}$ of the processes $p(\gamma,\pi^0\pi^0)p$ and $d(\gamma,\pi^0\pi^0)pn$ are seen. Dashed (solid) curves on the figure correspond to calculation without (with) diagram (17) (see Fig.(1)) inclusion.

As it can be see from the figure, sum of distributions $d\sigma/d\omega_{\pi\pi}$, separately calculated for proton and neutron (dotted curve on right panel of Fig.(5)), precisely reproduces experimental data in the region $\omega_{\pi\pi} \geq 330$ MeV.

In general, presented by the model a good agreement with experimental total cross sections for the processes $d(\gamma,\pi^0\pi^0)d$ and $d(\gamma,\pi^0\pi^0)pn$ (see Fig.(6)), is in coincidence with predictions of work [4]. Following this idea and also bearing in mind that total cross section on proton and deuteron in the processes $p(\gamma,\pi^0\pi^0)p$ and $d(\gamma,\pi^0\pi^0)pn$ are underestimated in second resonance region it can concludes that this circumstance in a less degree relates with 'missing' resonance problem. As it was demonstrated in the work, additional resonance and Born contributions – *a.c.* lead to a negligible effect in third resonance region. Moreover, double pion rescattering mechanism inclusion in the process $\pi^+\pi^- \to \pi^0\pi^0$ with purely parametrized amplitude in a wide pion energy region, does not reproduce experimental total cross section at $E_{\gamma} \leq 700$ MeV. At the same time it should be emphasized that simple Breit-Wigner's parametrization for the rescattering amplitude $f_{\pi\pi}$ in Eq.(6) leads to a marked increase of total cross section of $p(\gamma,\pi^0\pi^0)p$ near $E_{\gamma} = 500 - 550$ MeV, but in this case $f_{\pi\pi}$ poorly reproduces $s-$wave phase shifts of $\pi\pi$ scattering.

5. Conclusion

Total cross sections of $(\gamma,\pi^0\pi^0)$ processes on proton and deuteron were calculated in the work. Making up the reaction $(\gamma,\pi^0\pi^0)$ amplitudes includes information about baryon resonances on PDG-2014 [14] compilation. Besides, as applied to $p(\gamma,\pi^0\pi^0)p$ and $d(\gamma,\pi^0\pi^0)pn$ rescattering mechanism in $\pi^+\pi^- \to \pi^0\pi^0$ process is considered. As a result rescattering mechanism inclusion $\pi\pi$ amplitude of that is taken into account from [12] keeps out supply the total cross section underestimation in resonance region. At the same time rescattering effect is rated by Eq. (6) is seen to be in definite dependence on the off-shell part of $f_{\pi\pi}$ amplitude.

Acknowledgments

The author acknowledges support of Dynasty foundation, and Federal program 'Nauka' (project 825).

References

[1] Gomez Tejedor J A and Oset E 1996 *Nucl. Phys.* A **600** 413
[2] Murphy L Y and Laget J M 1996 Reaction mechanisms in two pion photoproduction on the proton: meson echange picture *Preprint* DAPNIA-SPHN/96-10
[3] Ochi K, Hirata M and Takaki T 1997 *Phys. Rev.* C **56** 1472
[4] Fix A and Arenhövel H 2005 *Eur. Phys. J.* A **25** 115
[5] Fix A and Arenhövel H 2013 *Phys. Rev.* C **87** 04503
[6] Egorov M and Fiks A 2011 *Russian Physics Journal* **54** 458
[7] Kondrashov A 1999 *Nucl. Phys. Proc. Suppl.* **74**, 180-185
[8] Alvarez-Ruso L, Oset E and Hernandez E 1998 *Nucl. Phys.* A **633** 519
[9] Muhlich P, Alvarez-Ruso L, Buss O and Mosel U 2004 *Phys. Lett.* B **595** 216
[10] Roca L, Oset E and Vicente Vacas M J 2002 *Phys. Lett.* B **541** 77
[11] Oset E, Roca L, Vicente Vacas M J and Nacher J C 2001 *Workshop of Chiral Fluctuations in Hadronic Matter*, September, Orsay, Two pion photoproduction on nucleons and nuclei in the rho and sigma regions
[12] García-Martin R, Kamiński R, Peláez J R, Ruiz de Elvira J, Ynduráin F G 2011 *Phys. Rev.* D **83** 074004

[13] Bjorken J and Drell S 1964 *Relativistic Quantum Mechanics* (McGraw-Hill: Springer)
[14] Olive K A, Agashe K, Amsler C, Antonelli M, Arguin J F, Asner D M, Baer H, Band H R, Banett R M, Basaglia T and *et al.* (Particle Data Groupe) 2014 *Chin. Phys.* C **38** 090001
[15] Manley D M and Saleski E M 1992 *Phys. Rev.* D **45** 4002
[16] Machleidt R, Holinde K and Elster C 1987 *Phys. Rep.* **149** 1
[17] Takamatsu K, Ma, A M, Ishida M Y, Ishida S, Ishida T, Tsuru T, Shimizu H, *et. al.* and (E135 Collaboration) 2000 *Nucl. Phys.* A **675** 312 (2000)
[18] Sarantsev A V, Fuchs M, Kotulla M, Tjoma U, Ahrens J, Annand J R M, Anisovich A V, Anton G, Bantes R, Bartholomy O and [*et. al.*], (CB-ELSA and A2-TAPS Collaborations) 2008 *Phys. Lett.* B **659** 94
[19] Kamalov S S and Oset E 1997 *Nucl. Phys.* A **625** 873
[20] Kashevarov V L, Fix A, Prakhov S, Aguar-Bartolomé P, Annand J R M, Arends J, Bantawa K, Beck R, Bekrenev V, Berghäuser H and [*et al.*] (Crystal Ball at MAMI, TAPS, and A2 Collaborations) 2012 *Phys. Rev.* C **85** 064610
[21] Assafiri Y, Bartalini O, Bellini V, Bocquet J P, Bouchigny S, Capogni M, Castoldi M, D'Angelo A, Didelez J P, Di Salvo R and [*et al.*] 2003 *Phys. Rev. Lett.* **90** 222001
[22] Messchendorp J G, Janssen S, Kotulla M, Ahrens J, Annand J R H, Beck R, Bloch F, Caselotti G, Fog L, Hornidge B and [*et al.*] 2002 *Phys. Rev, Lett.* **89** 222302
[23] Maghrbi Y, Gregor R, Lugert S, Ahrens J, Annand J R M, Arends H J, Beck R, Bekrenev V, Boillat B, Braghieri A and [*et al.*] 2013 *Phys. Lett.* B **722** 69
[24] Jaeglé I 2009 *CB Meeting*, September, Edinburgh, Photoproduction of multiple mesons off light nuclei
[25] Krusche B, Fuchs M, Metag V, Robig-Landau M, Stroher H, Beck R, Harter F, Hall S J and Kelle J D 1999 *Eur. Phys. J.* A **6** 309
[26] Kleber V, Achenbach P, Ahrens J, Beck R, hejny V, Kellie J D, Kotulla M, Krusche B, Kuhr V, Leukel R and [*et al.*] 2000 *Eur. Phys. J.* A **9** 1
[27] Benaksas D, Cosme G, Jean-Marie B, Jullian S, Laplanche F, Le Francois J, Liberman A D, Parrour G, Repellin J P, Sauvage G 1972 *Phys. Lett.* B **39** 289